Electronic Supplementary Material (ESI) for Nanoscale.
This journal is © The Royal Society of Chemistry 2015

Electronic Supporting Information

Highly Air Stable Passivation of Graphene Based Field Effect Devices

Abhay A. Sagade[*a], Daniel Neumaier*[*a], Daniel Schall*[a], Martin Otto*[a], Amaia Pesquera*[b], Alba Centeno*[b], Amaia Zurutuza Elorza*[b], and Heinrich Kurz*[a]*

[a]Advanced Microelectronic Center Aachen (AMICA), AMO GmbH, Otto-Blumenthal-Strasse 25, 52074, Aachen, Germany.

[b]Graphenea S.A. A75022608 Tolosa Hiribidea 76 20018 Donostia-San Sebastian, Spain.

*** Address corresponds to:** abhaysagade03@gmail.com, neumaier@amo.de

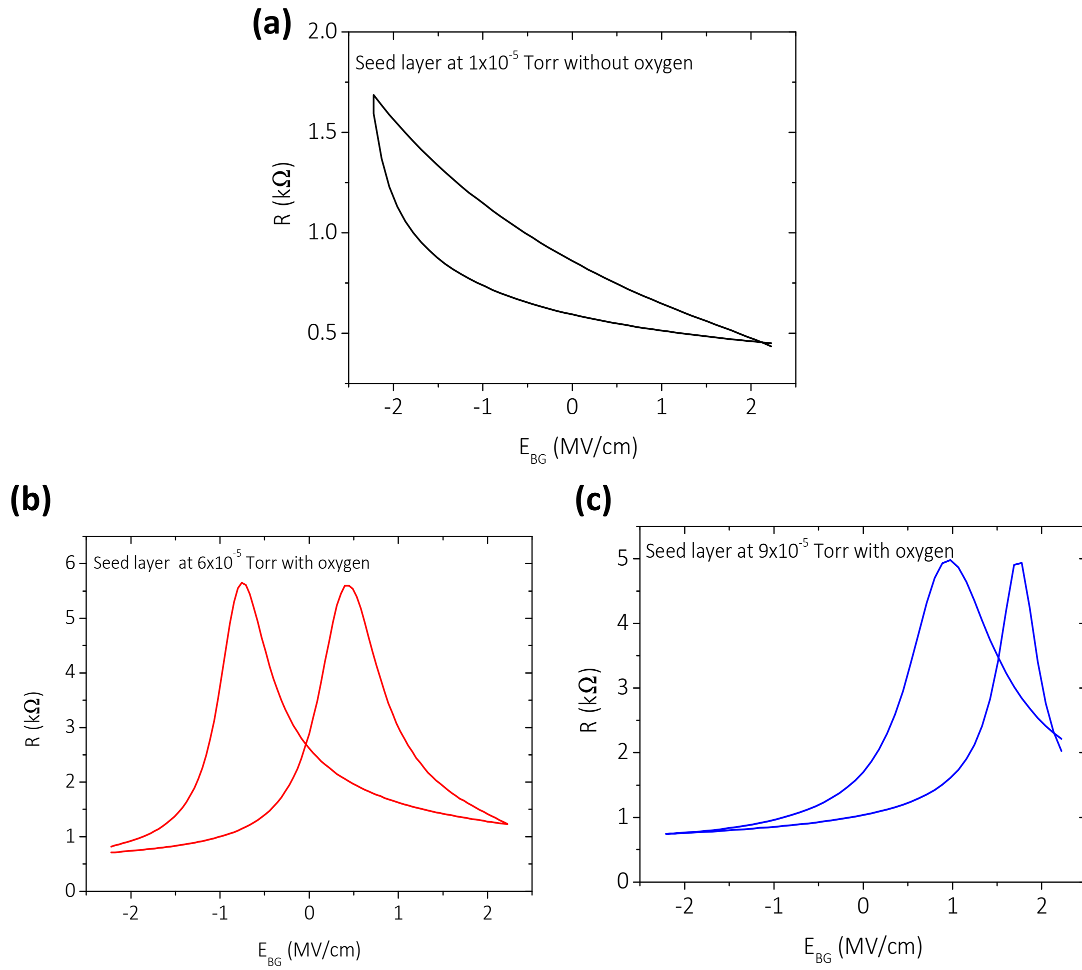

Fig. S1 The transfer characteristics of photo-lithographically fabricated Hall-bars after depositing three different seed layers as discussed in main text for Fig. 1, but before depositing 90 nm Al_2O_3. The measurements were carried out in air with V_{DS} = 50 mV.

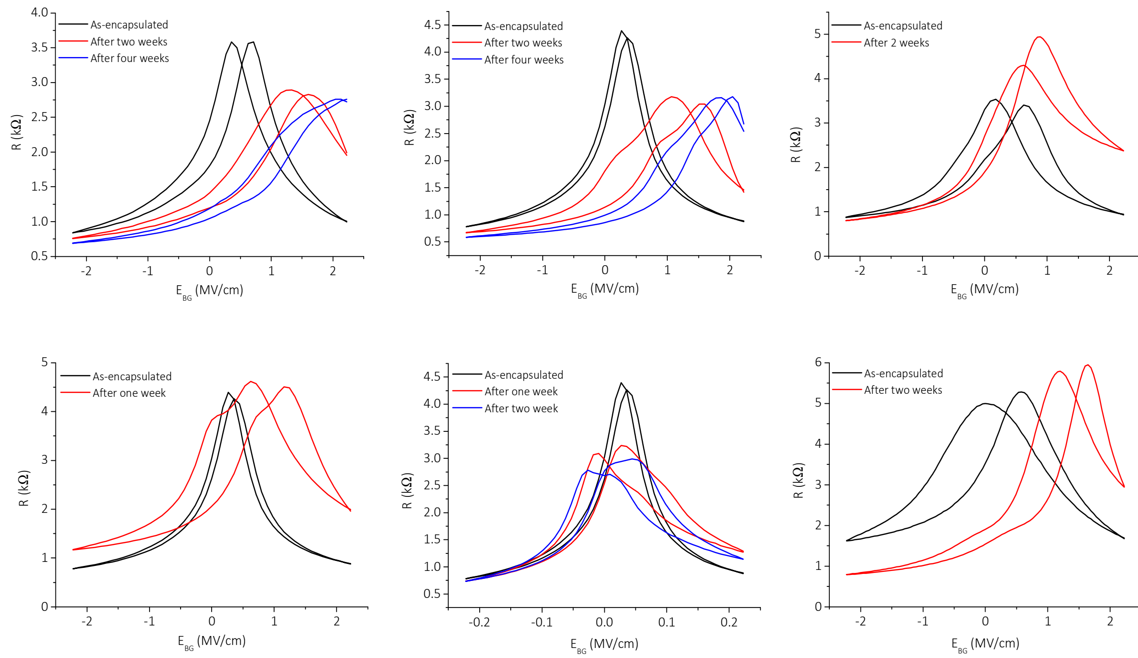

Fig. S2 In the study of different oxygen pressures, at 9x10^{-5} Torr two different chips with 3 working devices on each (in total 6) were investigated. The thickness of Al_2O_3 is 90 nm. Figure shows transfer curves of these devices with time. The device degradation pattern is random. It indicates that though the difference in the values of 6x10^{-5} Torr and 9x10^{-5} Torr pressure is small, it has significant effect on the growth process of oxide.

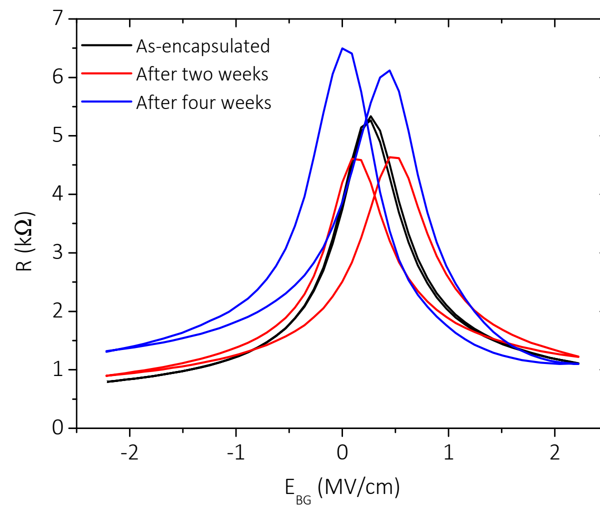

Fig. S3 The transfer characteristics of photo-lithographically fabricated Hall bar encapsulated with 60nm Al_2O_3 after depositing seed layer of *in-situ* oxidized Al by e-beam evaporation at 6×10^{-5} Torr. The as-encapsulated device shows similar device performance as shown in Fig. 1e in main paper, but due to insufficient thickness of encapsulation layer the negligible hysteresis increases with time.

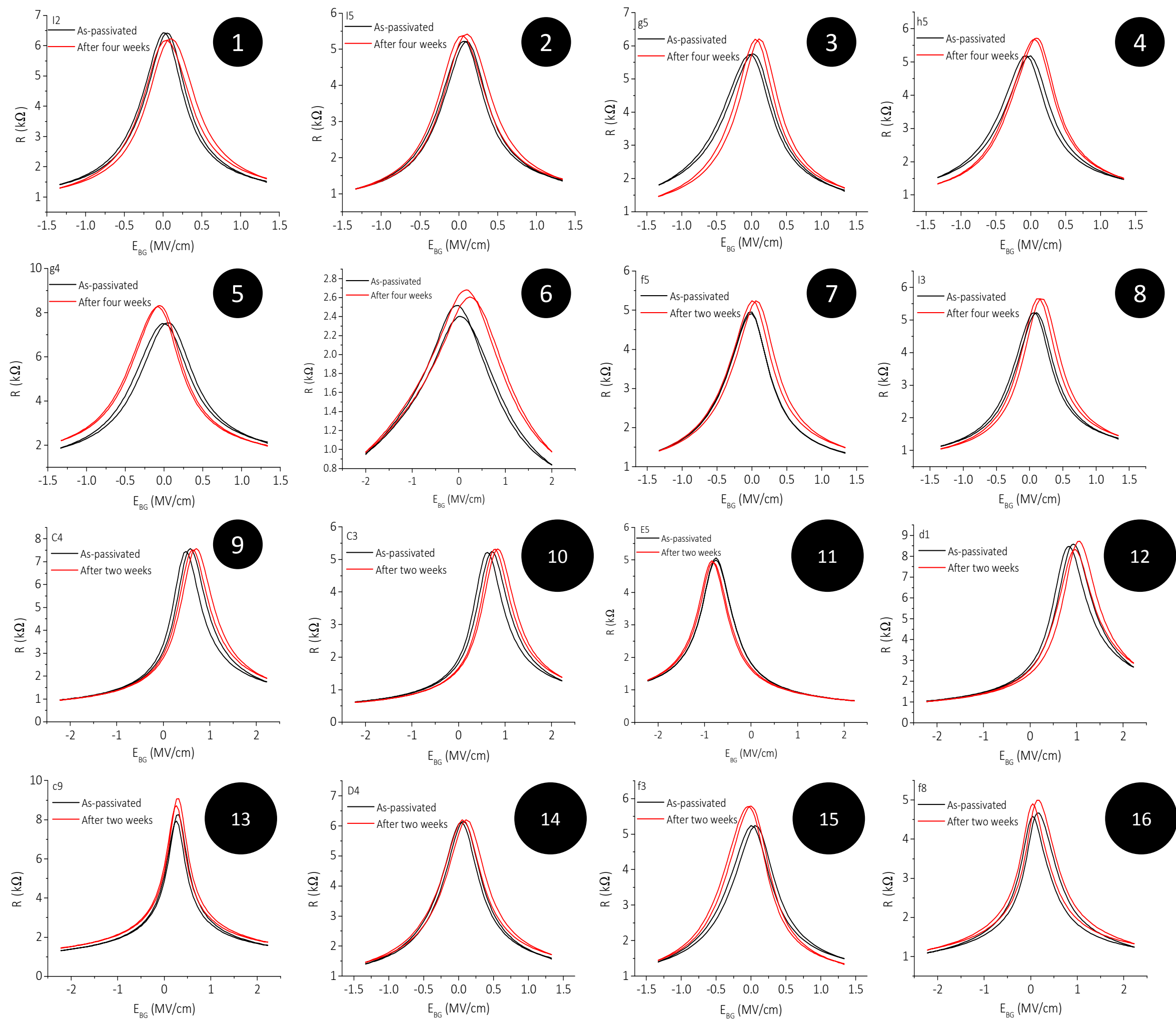

Fig. S4 Transfer curves of 17 devices (out of 20, rest 3 are shown in the main manuscript Figures 1e and 3b,c) studied for passivation using seed layer deposited at $6x10^{-5}$ Torr with oxygen and 90 nm Al_2O_3.

One chip with some of the devices (1-5,7,8) shown above was stored in air for six months and following plots shows consistent performance:

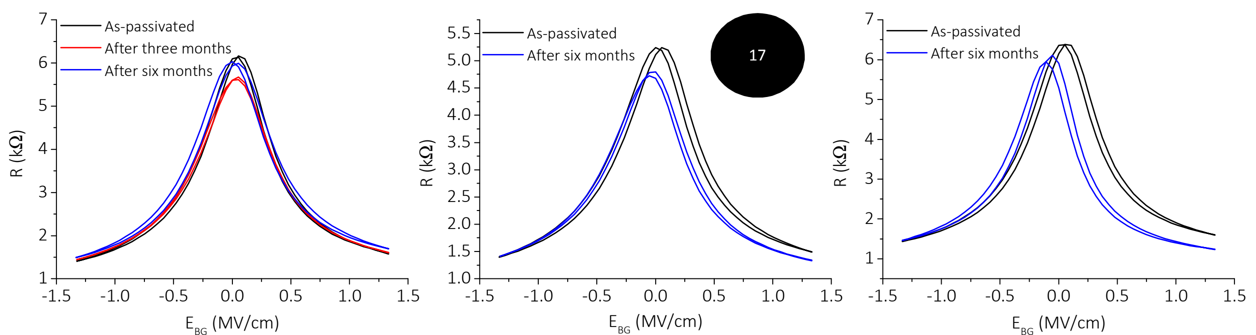

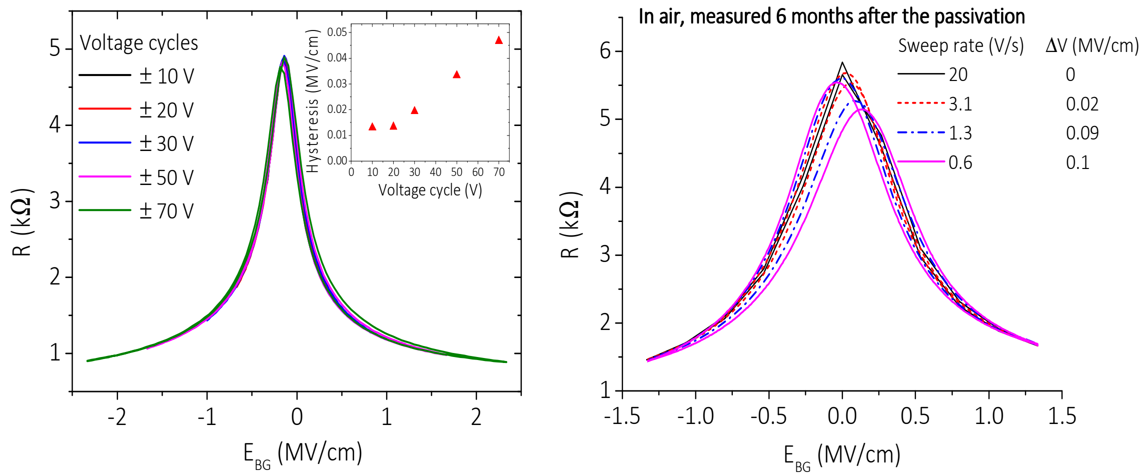

Fig. S5 Measurement of transfer curves at different voltage cycles (left) and sweep rates (right) for the passivated Hall-bars fabricated on 300nm SiO_2/Si. Inset shows the variation in the hysteresis with different voltage cycles. Here largest hysteresis observed at ±70V cycle was of 1.5V which translates to 0.05 MV/cm. While, the hysteresis is found to increase with decreasing sweep rate.

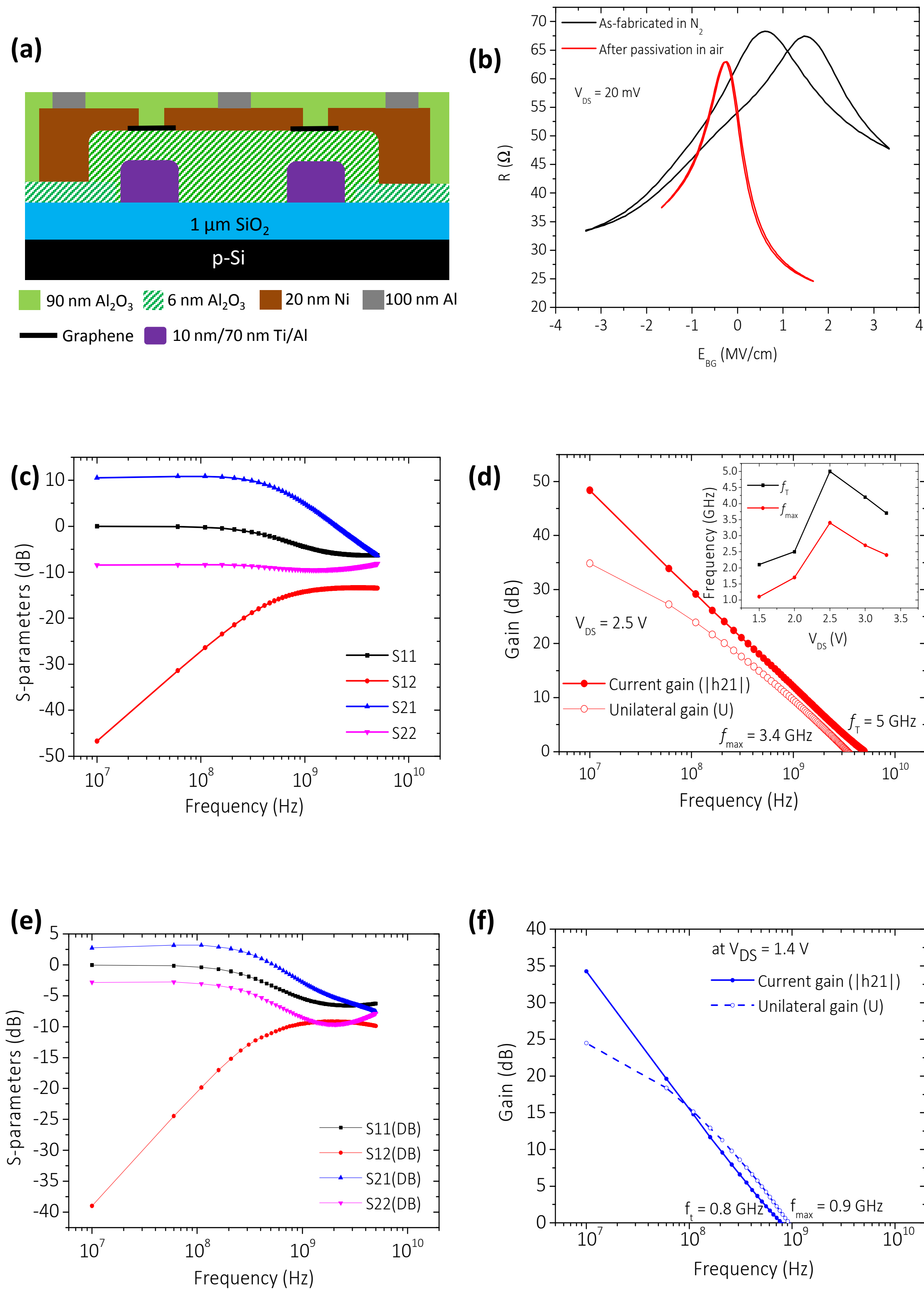

Fig. S6 (a) Schematic showing the layers of material used in fabrication of RF-transistor on solid and flexible substrate. The flexible devices were fabricated on 60 µm thick kepton sheet. The dimensions of the transistor were: channel length = 1.1 µm, channel width = 140 (2 × 70) µm, gate length = 3.5 µm on solid substrate and channel length = 5 µm, channel width = 140 (2 × 70) µm, gate length = 7 µm on flexible substrate. (b) The transfer characteristics of a transistor before and after passivation

on solid substrate. RF performance of transistor: (c), (d) and (e), (f) in terms of as-measured S-parameters and derived extrinsic current gain and unilateral gain for solid and flexible substrates, respectively. Inset in (d) shows variation of frequency response as a function of source-drain bias.

In one more case we demonstrate the passivation of graphene RF transistors. The transfer characteristics in Fig. S6b compares the device performance before and after passivation. The transconductance of the device is enhanced from 1.8 μS/μm before to 5.7 μS/μm after passivation at V_{DS} = 20 mV. Such threefold increment in transconductance and huge reduction in hysteresis after passivation is crucially beneficial for high frequency devices. Figures S6c-f shows RF performance of the passivated device in ambient. The forward gain (S21) shows a significant value of 11 dB for the channel width of 140 μm. This device showed extrinsic (without de-embedding) transit frequency (f_T) of 5 GHz and maximum oscillation frequency (f_{max}) of 3.4 GHz at V_{DS} = 2.5 V. This process technology is also compatible with flexible substrates. Though the observed frequency response of RF transistor is not the best performance compared to the top gated and e-beam fabricated state-of-the-art devices, this study showed that back gated device can be operated in air with the aid of passivation.

Table-T1: The values obtained for hysteresis and corresponding trap charge density (n_t = C_{ox} x $\Delta V_{Dirac}/q$) in the present study.

Figure number	Hysteresis (MV/cm)	Trap charge density (cm^{-2}) x 10^{10}
Fig. 1c	As-encapsulated: 0.44 After 2 weeks: 0.66 After 4 weeks: 0.66	85.6 128 128
Fig. 1e	As-encapsulated: 0.04 After 2 weeks: 0.08 After 4 weeks: 0.08	7.76 17.27 17.27
Fig. 1f	As-encapsulated: 0.26 After 2 weeks: 0.3	50.45 58.22
Fig. 3b	1st litho: negligible* 2nd litho: negligible 3rd litho: 0.04	negligible negligible 21.24
Fig. 3c	1st litho: negligible 3rd litho: 0.106 After vacuum storing: negligible	negligible 22.8 negligible

**During the measurements, the voltage step was of 0.2 V, therefore the value of ΔV_{Dirac} was not measured better than 0.006 MV/cm.*

Table-T2: Summary of the performance parameters for the devices shown in Fig. S4.

#Device	Field effect Mobility (cm^2/V.s)	$V_{BG} = V_{Dirac}$ (V)		Hysteresis (MV/cm)	
		As-passivated	With time	As-passivated	With time
1	1700	0.8	1.6	0.05	0.05
2	2000	2.4	1.6	0.02	0.05
3	1360	0	1.6	0.05	0.05
4	1585	-1.6	1.6	0.03	0.05
5	1140	0	-1.6	0.02	0.03
6	1500	0	4.8	0	0.08
7	1755	0	1.6	0	0.05
8	2050	2.4	3.2	0.02	0.05
9	1600	4.4	5.6	0.06	0.06
10	2420	5.6	6.8	0.06	0.06
11	2200	-7.2	-6.8	0	0.04
12	1300	7.6	8.8	0.08	0.08
13	1400	2.4	2.4	0	0
14	1600	0.8	1.6	0.02	0.05
15	1880	0	-0.8	0.05	0.02
16	1750	0.4	0.4	0.08	0.08
17	1720	0	-1.6	0.05	0.05
18	1120	-2.3	-1.17	0.04	0.04
19	1500	0	0	0	0
20	2700	-2.7	NA	0	NA

Table-T3: Comparison of hysteresis and corresponding trap charge density values obtained in the literature.

Sr. No.	**Publication**	**Device fabrication process and encapsulation employed**	**Hysteresis (MV/cm)**	**Trap charge density (cm^{-2}) x 10^{10}**
1	*ACS Nano* 4 (2010) 7221	E-beam Lithography. DC. No passivation, IN AMBIENT	0.5	107.8
2	*Carbon* 53 (2013) 182	Photolithography. DC. Al_2O_3 of 30nm at 130C, IN AMBIENT	2.2	431.2
3	*Carbon* 60 (2013) 453	Photolithography. Al_2O_3 of 30nm at 130C, IN AMBIENT DC PULSE	 0.4 0.2	 86.24 43.12
4	*Appl. Phys. Lett.* 103 (2013) 253505	E-beam Lithography. DC. PMMA of 1µm, IN N_2	0.16	36
5	*Nano Lett* 9 (2009) 422	E-beam Lithography. DC. Al_2O_3 of 12nm at 250C	0.16	36
6	*IEEE Trans. Electron Devices* 61 (2014) 1583	E-beam Lithography. Nanosecond pulsed measurement. Al_2O_3 of 20nm, IN AMBIENT	0.05	16.6
7	**Present work**	**Photolithography. DC.** **Al_2O_3 of 90nm at 150C, IN AMBIENT**	**0-0.08**	**0-17.27**

Table of content:

Graphene devices are sensitive to ambient conditions and hence the device performance is unstable. Here we report on the use of aluminum oxide (Al_2O_3) as passivation layer with *in-situ* oxidized aluminum seed layer on single layer graphene field effect devices which assists highly air stable device performance over several weeks.